Polymer 282 (2023) 126180

Contents lists available at ScienceDirect

Polymer

journal homepage: www.elsevier.com/locate/polymer

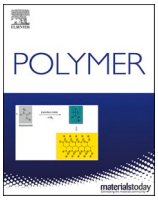

Surface-enhanced nucleation in immiscible polypropylene and polyethylene blends: The effect of polyethylene chain regularity

Magdalena Góra [a], Sebastián Coba-Daza [c], Enrico Carmeli [b], Davide Tranchida [b], Andreas Albrecht [b,**], Alejandro J. Müller [c,d,*], Dario Cavallo [a,***]

[a] Dipartimento di Chimica e Chimica Industriale, Università degli studi di Genova, via Dodecaneso 31, 16146, Genova, Italy
[b] Borealis Polyolefine GmbH, Innovation Headquarters, St. Peterstrasse 25, 4021, Linz, Austria
[c] POLYMAT and Department of Polymers and Advanced Materials: Physics, Chemistry and Technology, Faculty of Chemistry, University of the Basque Country UPV/EHU, Paseo Manuel de Lardizabal, 3, 20018, Donostia-San Sebastian, Spain
[d] IKERBASQUE, Basque Foundation for Science, Plaza Euskadi 5, 48009, Bilbao, Spain

A B S T R A C T

In blends where polyethylene (PE) is the minor component dispersed in an isotactic-polypropylene (PP) matrix, an enhancement of the crystallization rate of PE was found when the crystallization temperature of the matrix phase is increased by means of a self-nucleation protocol. Such an effect is interpreted as the result of the epitaxial nucleation of PE droplet domains at the interface with the PP matrix (*Macromolecules*, **2021**, 54, 19, 9100–9112). This study extends the findings on immiscible blends of a PP matrix and various industrially produced PE grades as the dispersed phase. Eight different PEs with varying molecular architecture, and thus density and melting temperatures, were mixed with PP in a 20/80 PE/PP weight ratio. The possible existence of surface nucleation was probed by applying a self-nucleation thermal protocol to the PP matrix and recording the concomitant variation of PE crystallization temperature (T_c). Different behaviours are observed for various PEs. In particular, those with relatively high density display a clear increase in crystallization temperature, over 3.0 °C, when the T_c of the matrix is increased (i.e., as PP lamellar thickness increased), indicating an efficient surface nucleation mechanism. Metallocene-made LLDPE also shows a small increase, about 1.7 °C, while PEs with lower densities, below 927 kg/m^3, metallocene PEs or LDPE display no meaningful change in T_c with matrix self-nucleation. It was demonstrated that a threshold value of chain regularity is required to trigger the surface nucleation of PE on PP. Only polymers with a density above approximately 920 kg/m^3 and melting temperatures exceeding about 115 °C can efficiently nucleate onto the PP substrate. It is postulated that the presence of a high amount of branches or comonomers along the PE chains hinders the epitaxial matching between PE and PP.

1. Introduction

Nucleation is a fundamental step of crystallization, consisting of the aggregation of molecules to form supercritical size clusters, whose further growth into a macroscopic crystal is spontaneous [1,2]. In semicrystalline polymers, controlling nucleation is of great importance, for instance, to tune mechanical and optical properties [3]. Typically, polymer nucleation occurs on the surface of a heterogeneous substance due to the lower energy barrier in comparison with homogenous nucleation. Of particular interest is the nucleation of one polymer to another, which becomes extremely efficient if the two polymers exhibit some degree of lattice matching between their crystalline structures. This latter case is known as epitaxy. Systematic investigations about epitaxy in the polymer field have been reported by Lotz and Yan [4–6].

A well-studied example is the nucleation of high-density polyethylene (HDPE) on isotactic polypropylene surfaces (PP) [7–10]. It was shown for model systems in oriented thin films and blends that polyethylene (PE) chains crystallize with an angle of 50° with respect to the PP chain axis. This can be explained due to the alignment of the zig-zag PE chain along the rows of PP methyl groups having 0.5 nm intermolecular distances between the chain-row matches [7].

Yan and Petermann studied the effect of polyethylenes of various chain regularity and, therefore different PE densities on epitaxial nucleation onto an oriented PP substrate [11]. They analysed the behaviour of high-density polyethylene (HDPE), linear low-density polyethylene (LLDPE) low-density polyethylene (LDPE). They found that all three PEs show epitaxial crystallization on PP according to the known crystallographic relationship for HDPE. However, the thickness

* Corresponding author. POLYMAT and Department of Polymers and Advanced Materials: Physics, Chemistry and Technology, Faculty of Chemistry, University of the Basque Country UPV/EHU, Paseo Manuel de Lardizabal, 3, 20018, Donostia-San Sebastian, Spain.
** Corresponding author.
*** Corresponding author.
E-mail addresses: andreas.albrecht@borealisgroup.com (A. Albrecht), alejandrojesus.muller@ehu.es (A.J. Müller), dario.cavallo@unige.it (D. Cavallo).

https://doi.org/10.1016/j.polymer.2023.126180
Received 31 March 2023; Received in revised form 13 June 2023; Accepted 4 July 2023
Available online 5 July 2023

Table 1
List of the used materials in the investigation with material designation code, density and results from DSC and GPC measurements.

Material designation	Density[a] [kg/m^3]	Comonomer content [wt %]	Comonomer type	T_m [°C]	T_c [°C]	χ_c [%]	M_w [kg/mol]	$Đ$
PP	905	–	–	161.1	112.4	52%	342.0	8.4
ZNPE962	962	C4	0.7	132.7	119.4	83%	67.8	3.8
ZNPE954	954	C4	1.1	128.7	116.2	74%	90.2	10.4
ZNPE945	945	C4	2.1	128.1	115.5	68%	158.5	16.0
ZNPE935	935	C4	4.8	127.3	114.8	57%	206.0	19.8
mPE927	927	C6	4.6	119.5	106.5	46%	77.7	3.8
LDPE922	922	–	–	112.7	97.8	45%	101.5	6.7
mPE918	918	C4/C6	0.6/7.5	121.9	107.0	41%	91.6	3.7
mPE902	902	C8	17.0	94.5	77.5	27%	52.8	3.5

C4 = 1-butene.
C6 = 1-hexene.
C8 = 1-octene.
[a] Datasheet.

of the epitaxially crystallized layer decreased from 250 nm to 30 nm as the polymer density lowered. This reduced thickness resulted from a competition between oriented and spherulitic growth in the film, although the authors did not suggest it, this effect could be explained by a slower epitaxial nucleation for more irregular polymers.

To study polymer-on-polymer nucleation kinetics, our group has devised a strategy applicable to binary polymer blends with two semicrystalline components and a droplet-in-matrix morphology [12,13]. The overall crystallization kinetics is dominated by nucleation in blends with a minor component dispersed as droplets in an immiscible matrix [14–17]. The method is based on differential scanning calorimetry (DSC) and consists in determining the relationship between the crystallization temperatures of the matrix and the dispersed phase when the matrix's T_c is varied through a self-nucleation thermal protocol [18]. The increase of matrix T_c due to self-nucleation enhances the dispersed phase T_c. This effect is attributed to the thicker crystalline lamellae of the matrix polymer, which provide a more favourable nucleation substrate to the droplet phase. The technique has been applied to various double semicrystalline polymer blends [12,13,19], including HDPE/PP [12], for which the epitaxial nucleation mechanism is active.

So far, the study is limited to the case of high-density polyethylene, and little is known about the applicability of such a method to PEs with different chain architecture (comonomer type and content and branching).

Much information is available on the effect of blending different types of PE with polypropylene, especially from the point of view of the adhesion between the phases in blends and laminates [20–22]. It is known that better welding is obtained with metallocene PEs rather than with Ziegler-Natta type polymers due to the segregation of low molar mass and defective chains to the interface in the latter case [20]. Improved adhesion was obtained when interfacial entanglements were formed (for lower density metallocene PEs) [21] or when crystallization across the interface occurred [22].

Despite the body of literature on interfacial morphology in blends of different PE types with PP, a specific study on nucleation kinetics at the interface has yet to be performed. The aim of the present study is thus to extend our versatile DSC method to the investigation of surface nucleation of PE on PP in immiscible blends with droplets-in-matrix morphology, exploring polyethylenes with different chain regularity and composition [13].

2. Materials and methods

An isotactic polypropylene produced with Ziegler-Natta catalyst technology with a molecular weight of 342.0 kg/mol was used as a matrix polymer for all investigated blends. The blends were prepared in a ratio of 80:20 polypropylene phase to polyethylene phase. The minor phase of each blend was composed of a different grade of polyethylene, including four Ziegler-Natta polyethylene (ZNPE) grades with varying density and molecular weight, three metallocene catalyst (mPE) grades with different comonomer types, and one low-density polyethylene (LDPE) from radical polymerization. The properties of all the used grades, measured as described below, are gathered in Table 1, together with the code names of the used PEs. In the sample name, the type of PE was followed by a number that represents the density of the material.

2.1. GPC

The molecular weight (Mw) was determined by Gel Permeation Chromatography (GPC) measurements using a GPC-IR chromatograph from PolymerChar (Valencia, Spain), equipped with an IR5 detector. The analysis was carried out at 160 °C and using three PLgel Olexis columns, each 300 × 7.5 mm (Agilent, Church Stretton, UK) as stationary phase. 1,2,4-Trichlorobenzene (TCB) was used as eluent with a flow rate of 1 mL/min. The column set was calibrated with narrow distributed polystyrene standards ranging from 500 to 11.5·10^6 g/mol. The PS equivalent molecular weight was converted into PE and PP equivalent by using Mark Houwink constants [23].

2.2. a-TREF

The chemical composition distribution (CCD) was analysed using a Crystaf-TREF 200+ PolymerChar instrument with an infrared concentration detector. 80 mg of sample was dissolved in 35 mL of trichlorobenzene (TCB), stabilized with 250 mg/L 2,6-bis(1,1-dimethylethyl)-4-methylphenol, at 160 °C. 0.3 mL of the solution was injected into the Temperature Rising Elution Fractionation (TREF) column. The column oven was cooled to 110 °C and held at 110 °C for 30 min for stabilization purposes. After stabilization, the column oven was cooled to 35 °C under a constant cooling rate (0.1 °C/min). The polymer was subsequently eluted from the column with 1,2,4-trichlorobenzene at a flow rate of 0.5 mL/min at 35 °C for a period of 10 min followed by a temperature increase from 35 °C to 140 °C at a constant heating rate of 0.5 °C/min with a flow rate of 0.5 mL/min. The concentration of the eluted fraction was determined by the detector and plotted as a function of temperature. TREF plots can be found in Fig. S1 of the supporting information and the extracted contents for the various fractions are collected in Table S1.

2.3. Self-nucleation thermal protocol (DSC)

To investigate the crystallization of the PE phase in relation to the change in the crystalline state of PP, the blends underwent a specific thermal protocol with a heating/cooling rate of 10 °C/min [12,13]. The polypropylene crystalline structure was altered through this thermal treatment, conducted on a Differential Scanning Calorimeter at various self-nucleation temperatures (T_s), as its crystallization temperature can be elevated through self-nucleation. The thermal protocol used to study

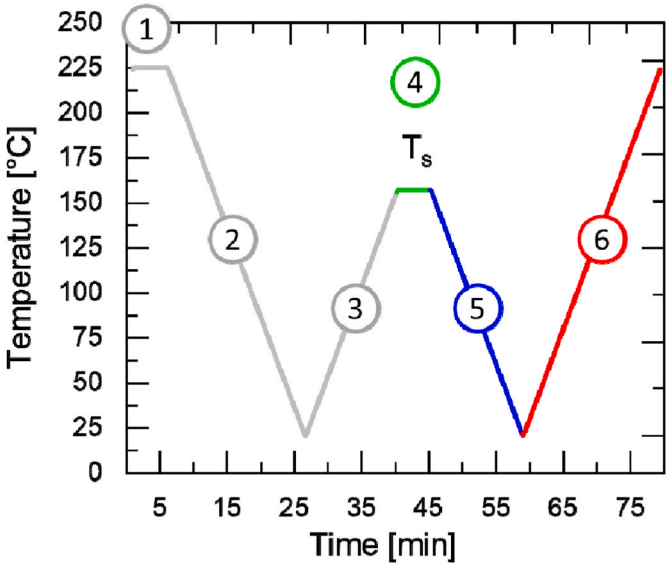

Fig. 1. Thermal protocol for performing PP matrix self-nucleation and crystallization of the dispersed phase.

Table 2
Thermal properties of blended materials obtained by DSC for each phase. The weight ratio in every blend is the same (80:20 PP:PE). The code of the blend therefore just indicates the difference in the type of PE.

Blend code	T_m^{PE} [°C]	T_c^{PE} [°C]	T_m^{PP} [°C]	T_c^{PP} [°C]
PP/ZNPE962	126.9	117.5	160.9	117.5
PP/ZNPE954	128.3	116.5	160.4	116.5
PP/ZNPE945	127.2	116.8	160.1	116.8
PP/ZNPE935	126.4	115.8	160.1	115.8
PP/mPE927	121.1	116.7	163.7	116.7
PP/LDPE922	110.2	98.8	160.2	113.9
PP/mPE918	121.5	114.4	160.5	114.4
PP/mPE902	94.7	80.3	160.9	114.7

the self-nucleation of the polypropylene matrix (Fig. 1) was adapted from Fillon et al. [18,24,25] and implemented as follows:

1. to erase thermal history, the sample was heated to 225 °C and held there for 5 min;
2. the sample was cooled to 20 °C at 10 °C/min to produce a standard crystalline state;
3. a heating scan at 10 °C/min was performed to a temperature denoted as T_s or self-nucleation temperature. Depending on the applied T_s, the different self-nucleation *Domains* of the material are revealed;
4. the sample was held at T_s for 5 min;
5. a cooling scan at 10 °C/min from T_s to 20 °C was performed;
6. a final heating scan at 10 °C/min from 20 °C to 225 °C was carried out to investigate the melting behaviour of both phases.

An analogous protocol, with additional lower T_s temperatures, was applied to all the neat PE grades.

2.4. Standard thermal protocol (DSC)

Melting (T_m) and crystallization (T_c) temperatures were measured using a Differential Scanning Calorimeter (DSC) Discovery series TA Instruments, according to ISO 11357/3. The measurements were carried out at a heating and cooling rate of 10 °C/min from 20 °C to 225 °C. The transitions were deduced from the second heating and cooling curves; the values of T_c and T_m are included in Table 1 and Table 2. The DSC curves are presented in Fig. 2 a) and b) for the neat PE grades and Fig. 2 c) and d) for the blends and neat PP.

2.5. Melt-mixing

Pellets from each selected PE grade were dry blended with polypropylene pellets in a weight ratio of PP/PE 80:20, and the resulting pellets mixtures were poured into the mixing chamber of a Brabender W50. Melt mixing was performed at a set temperature of 200 °C for 7 min at 100 rpm. The blends' composition code and basic thermal properties, measured by the DSC, are listed in Table 2 and presented in Fig. 2 c) and d).

2.6. SEM

Scanning electron microscopy (SEM) was used to visualize the general morphology of the blends and the interface between PP and PE. At first, the samples were conditioned in the DSC, applying annealing at the selected T_s and cooling to room temperature (i.e., steps 1 to 5 in Fig. 1). The selected samples were cut via cryo-microtoming at −100 °C on a Leica EM UC7 and then etched for 10 min in a 1% KMnO4 in 85% H_2SO_4 solution. After, the samples were washed with distilled water, stirred for 10 min in a 30% H_2O_2 solution, washed again, and finally rinsed with acetone. Before scanning electron microscope (SEM) analysis, the specimens were covered with a Pt layer using a Quorum Q150T S plus. SEM observations were performed on a Quanta 200F scanning electron microscope apparatus operating at an accelerating voltage of 5 kV.

3. Results and discussion

The present study examines the crystallization effect in blends of polypropylene and different types of polyethylene. To better understand the properties of the PE grades before melt-mixing with PP, we first conduct a basic analysis of each neat material. The self-nucleation properties of the PP matrix are then discussed, followed by an examination of the behaviour of the PE grades as the minor phase in the blend. Finally, the study aims to establish a correlation between the PE crystallization temperature after the thermal treatment and its molecular characteristics, namely the T_m and the methylene sequence length.

In this study, we utilized different grades of PE within a wide range of densities (from 902 to 962 kg/m^3), also featuring diverse molecular architecture of the polymer chains. This is reflected by a distinct crystallization behaviour of the polymers that can be seen in Fig. 2a–b, where the DSC cooling and subsequent heating curves of the various PE are reported. The crystallization and melting temperatures continuously drop 40 °C when decreasing the PE density from 962 to 902 kg/m^3. An exception to the observed trend is the behaviour of mPE918, which shows crystallization and melting temperatures higher than those of the LDPE with higher nominal density. The reason behind this observation will be discussed below.

Regarding the molecular features, ZNPE962 is characterized by a low weight-average molecular weight and extremely low comonomer content (T_m = 132.7 °C, M_w = 67.8 kg/mol, $Đ$ = 3.8) and therefore has higher crystallinity. The ZNPE962, ZNPE954, ZNPE945, and ZNPE935 are produced using the same catalyst technology, but the level of comonomer incorporation and the M_w differs. The radical polymerized grade LDPE922 has a high molecular weight and broad dispersity. The rest of the investigated grades are produced by single-site catalyst with a similar dispersity of ~3.7. Typical polymer chains produced under steady-state conditions by single-site catalysts (mPE927, mPE902) also possess an even comonomer concentration over the molecular weight distribution and random comonomer incorporation. A different situation holds for grade mPE918, whose TREF trace is reported in Fig. S1. Two chain populations characterized by a different comonomer concentration and hence elution temperature are visible.

The estimation of crystallinity was based on Equation (1), where

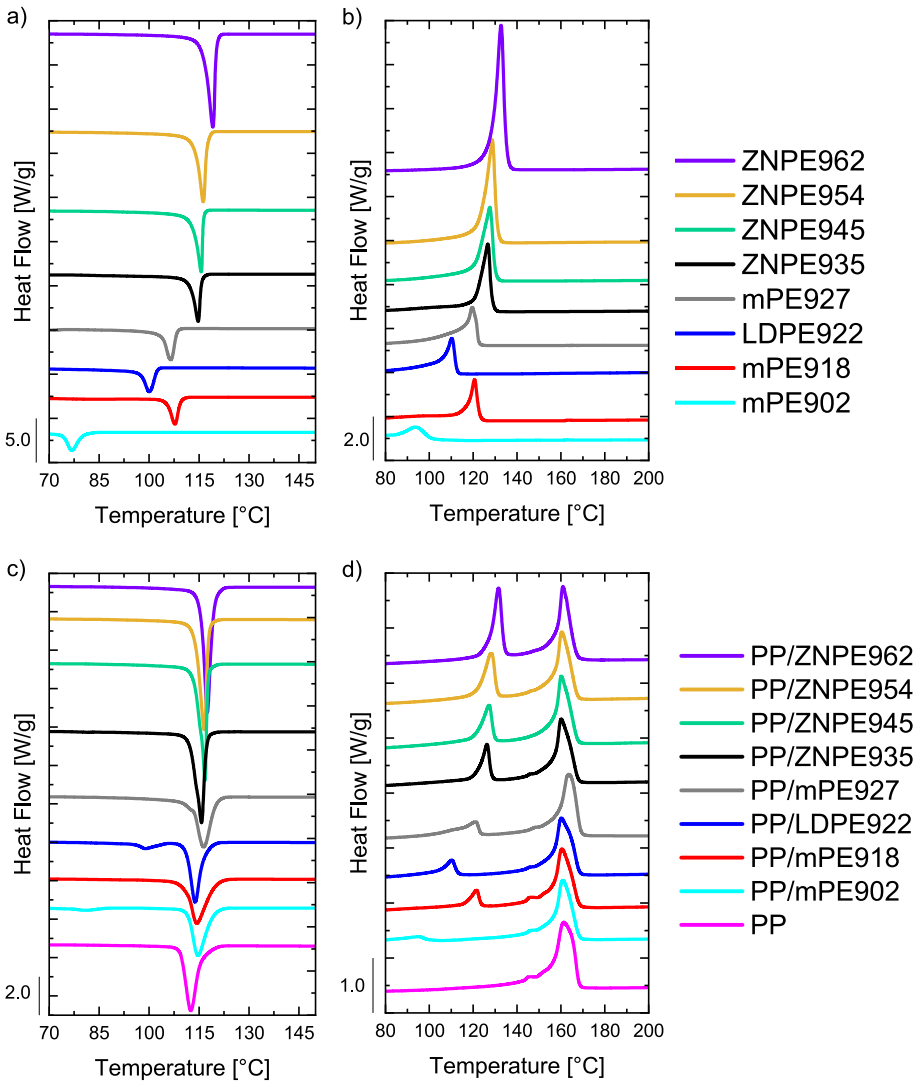

Fig. 2. DSC cooling (a) and heating (b) scans of neat PE grades and blends (c and d) at scan rates of 10 °C/min. The neat PE materials are arranged in order of increasing density from bottom to top and neat PP is added to the blends plot for comparison purposes.

ΔH_m^{ref} is a melting enthalpy of 100% crystalline polymer and ΔH_m is the experimental melting enthalpy. ΔH_m^{ref} for polypropylene is taken as 207 J/g [26,27] and for polyethylene 293 J/g [28,29], both generally accepted values.

$$\chi_c = \frac{\Delta H_m}{\Delta H_m^{ref}} \bullet 100 \quad (1)$$

Prepared blends with a ratio PP:PE equal to 80:20 were tested with the DSC, and the results are shown in Fig. 2c–d. The standard cooling and heating runs revealed a single transition during cooling for most of the blends, indicating coincident crystallization of the PP and PE phases, while just two blends present two separated crystallization peaks for the two phases (PP/LDPE922 and PP/mPE902). Polypropylene and polyethylene are known to display mutual nucleation effects [30–33]. Nevertheless, Fig. 2c shows that crystallization of the PP phase in the blends must occur at a higher temperature than for neat PP. The higher crystallization temperature of the PP phase in the blends can be explained by either a mild nucleating effect of the molten PE droplet for the PE grades whose density is below 935 kg/m^3 [33] or by nucleation onto the already formed PE crystals, especially for PEs with a density from 962 to 935 kg/m^3. Another possible explanation is the transfer of nucleating impurities from the PE to the PP phase during melt mixing, although the opposite transfer is more commonly observed [34–36]. It should be noted that for the blends for which the PE crystallization temperature could be measured during standard cooling, higher T_c values in comparison with neat polymers were detected. For example, mPE902 crystallization goes from 77.5 °C in the neat polymer to 80.3 °C in the blend and LDPE from 97.8 °C to 98.8 °C. This increase could indicate either nucleation of the PE phase at the interface with PP, the occurrence of which will be discussed in detail further on, or the transfer of nucleating impurities from the matrix to the dispersed phase [36].

As expected, the melting scans revealed the presence of two components (Fig. 2d). When comparing the melting temperature values of the PP and PE phases in the blend respect to the neat polymers, it is observed that the values tend to be slightly lower in the blend, which can be attributed to the effect of processing or different crystallization conditions [37,38].

In addition to these DSC results, we conducted an analysis using Wide Angle X-ray Scattering (WAXS) to delve deeper into the crystalline structure of the blends and neat materials. These WAXS measurements are detailed in the supporting information (Fig. S5). In brief, these results align with and corroborates the DSC data, displaying, for the different neat PE grades a crystallinity which continuously decreases with decreasing the nominal polymer density.

SEM images (Fig. 3) reveal that all blends display a sea-island morphology, with droplets of PE dispersed in the PP matrix. The PE

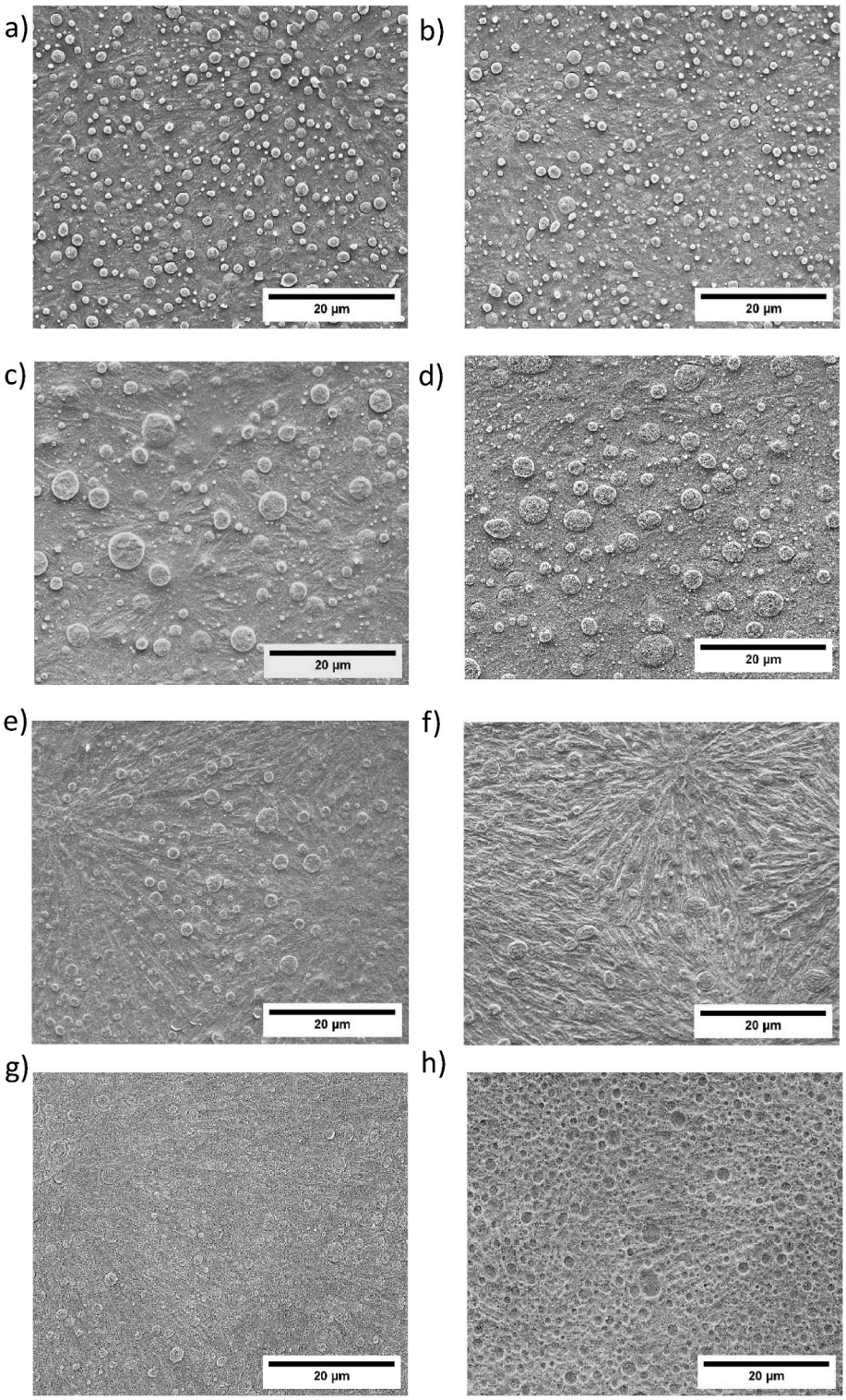

Fig. 3. Scanning electron microscopy images of a) PP/ZNPE962 b) PP/ZNPE954 c) PP/ZNPE945 d) PP/ZNPE935 e) PP/mPE27 f) PP/LDPE922 g) PP/mPE918 h) PP/mPE902.

droplet's size and size distribution (see Supporting Information, Fig. S2 and Table S2) vary only slightly. Still, it is important to note that the observed sizes are based on 2D images and may not accurately reflect the true size distribution of the 3D droplets. Even a monodisperse distribution of 3D particles would show a quite large distribution of sizes in a 2D image, with the largest diameter being the "true" diameter of the spheres. The differences in PE to PP viscosity ratio for the particular PE grades may contribute to the observed variation in droplet size. For instance, ZNPE935 generates a higher number of smaller droplets, while ZNPE945 yields a significant fraction of larger droplets. It is also worth noting that Fig. 3h) shows a region of the sample where the mPE902 material has been removed during the etching process. In this area, there are no visible PE droplets, and the diameter of the etched hole has been considered equal to the size of the PE droplets.

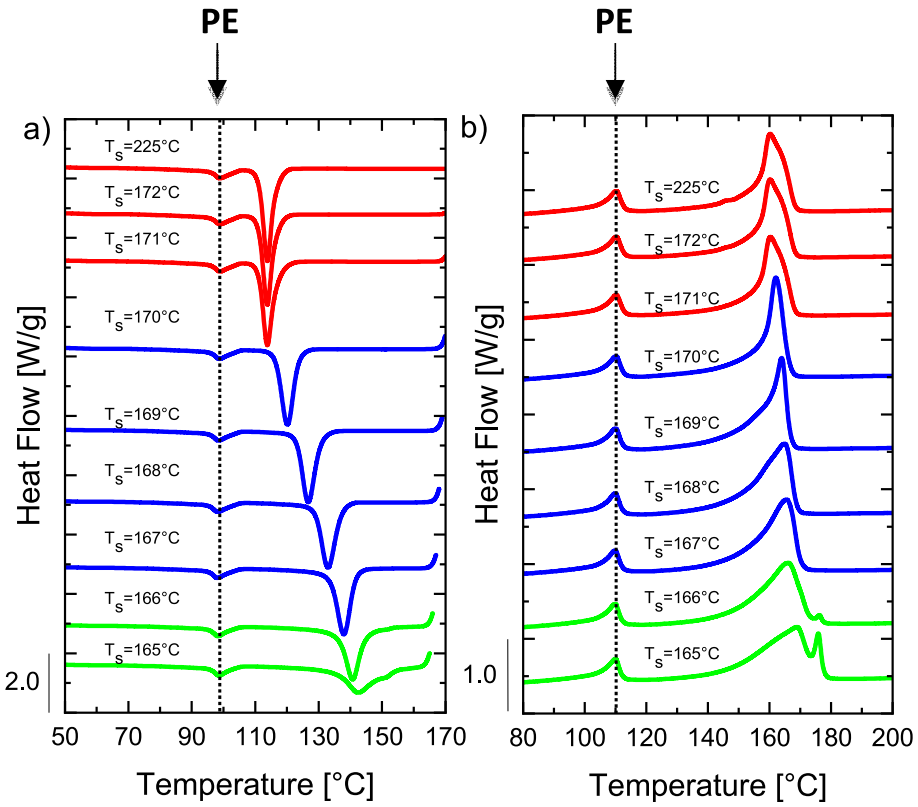

Fig. 4. DSC scans of a) cooling and b) heating after thermal treatment at the indicated T_s for the blend PP/LDPE922-80/20. Domain I is represented in red color, Domain II in blue and Domain III in green. Vertical dashed lines are added as a guide to the eye, to highlight the lack of changes in the crystallization temperature of the PE phase. (For interpretation of the references to color in this figure legend, the reader is referred to the Web version of this article.)

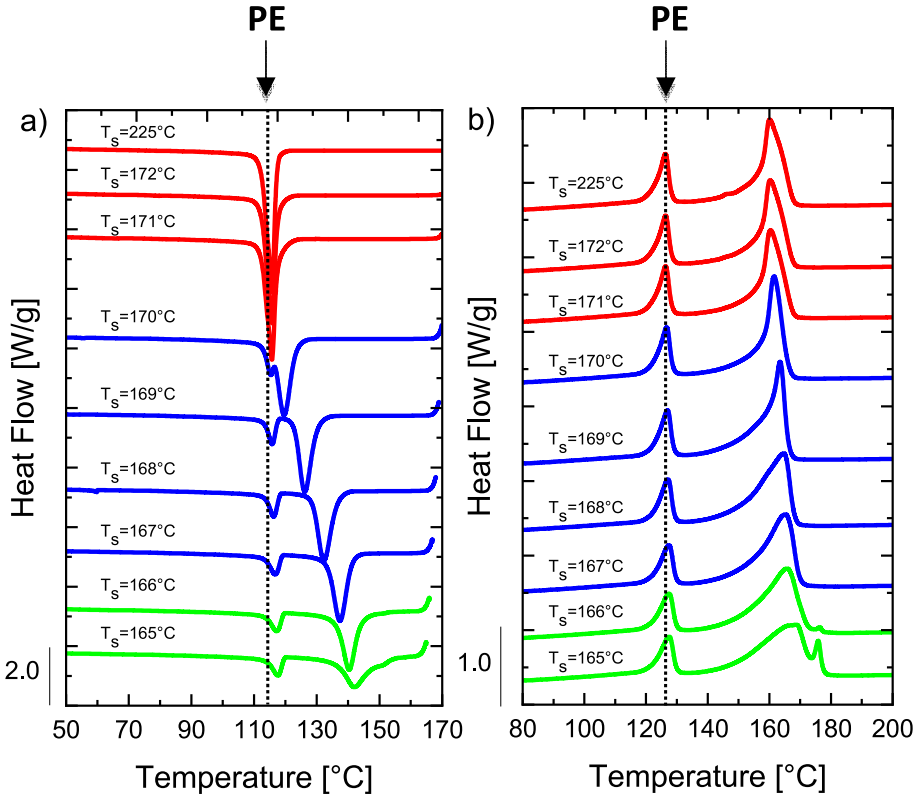

Fig. 5. DSC scans of a) cooling and b) heating after thermal treatment at the indicated T_s for the blend PP/ZNPE935. Domain I is represented in red color, Domain II in blue and Domain III in green. Vertical dashed lines are added as a guide to the eye, to highlight the changes in the crystallization temperature of the PE phase. (For interpretation of the references to color in this figure legend, the reader is referred to the Web version of this article.)

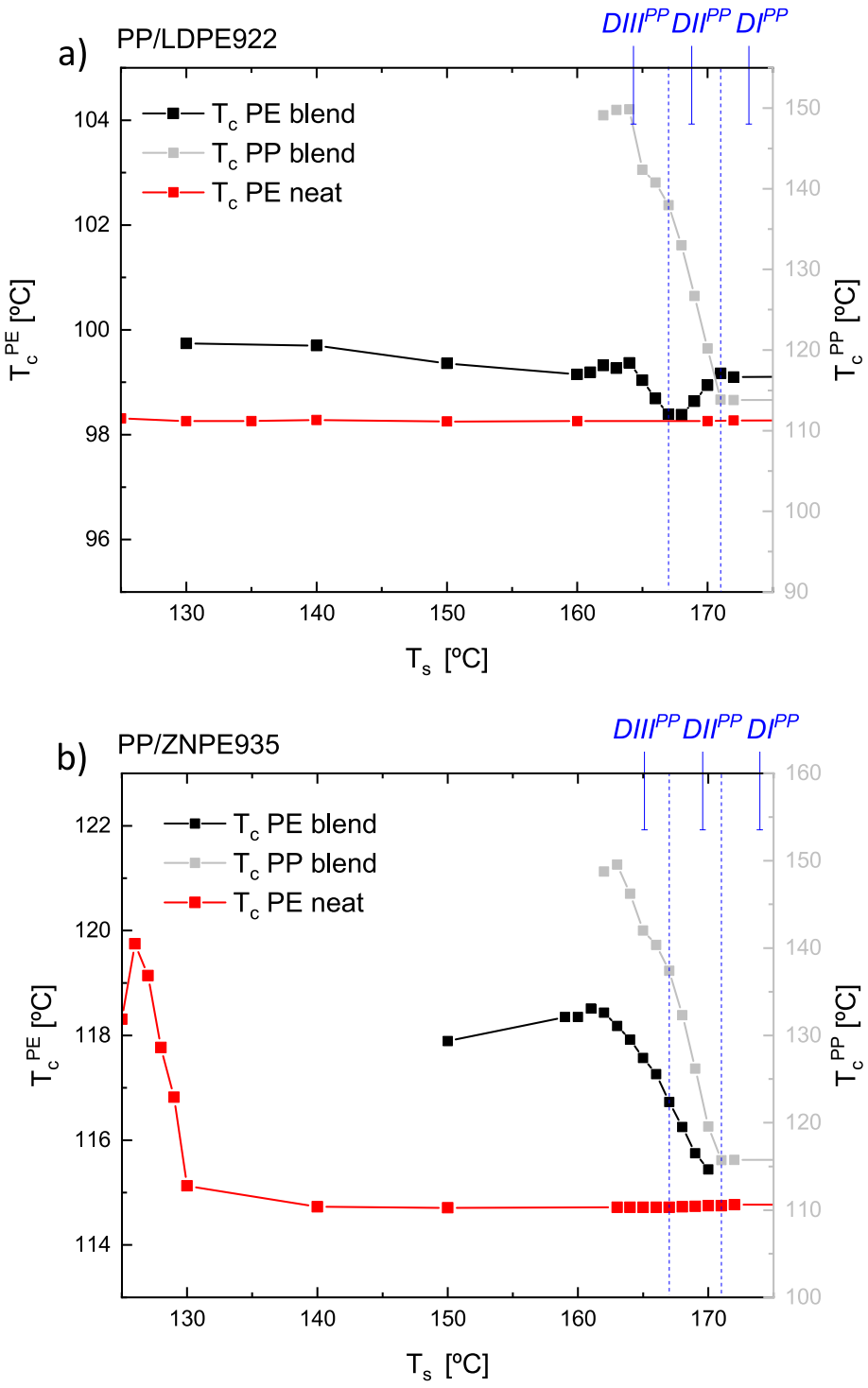

Fig. 6. Crystallization temperature (T_c) values of PE phase in the blend (black symbols, left y-axis) and PP phase (grey symbols, right y-axis) and of neat PE (red symbols) as a function of T_s for a) PP/LDPE922; b) PP/ZNPE935; The different self-nucleation Domains of PP are also indicated. (For interpretation of the references to color in this figure legend, the reader is referred to the Web version of this article.)

The measurement of PE droplet sizes displayed in Table S2 was performed according to Arnal et al. [39] and Chandrasekhar et al. [40]. It can be considered that the average diameter of the droplets in the blends is between approximately 1 and 2 μm. This suggests that the dimension of the various droplets with different PE types, being almost constant, will not affect the interpretation of the subsequent crystallization results.

Next, we investigated the interfacial nucleation of PE droplets on the self-nucleated PP matrix. As mentioned in the method section, the different self-nucleation *Domains*, depending on the applied T_s, are identified as follows: *Domain I*, at high enough T_s, is characterized by no effect on the material's recrystallization due to the complete erasure of any memory of the previous crystalline order; *Domain II*, at intermediate T_s, occurs when an enhanced crystallization temperature is recorded due to the presence of residual self-nuclei; *Domain III*, at lower T_s, is found when unmolten crystals are left in the original sample and the lamellae thicken as an effect of the heat treatment. It was shown for PP/PE blends that applying T_s in *Domain II* and *III* causes an increase in the

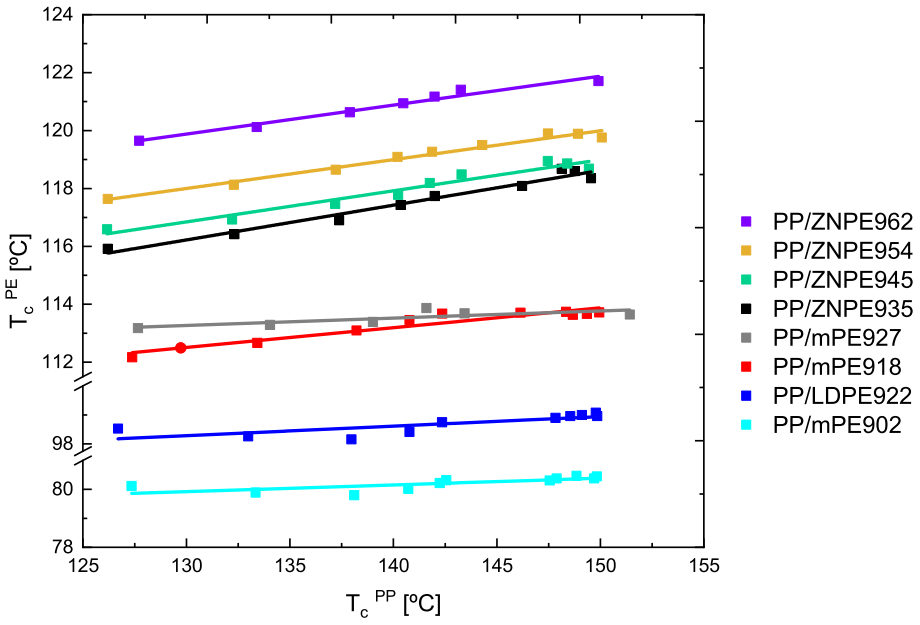

Fig. 7. T_c values of the PE as a function of T_c values of PP in the different blends. The lines are linear fitting of the data.

recrystallized PP lamellar thickness, which promotes epitaxial nucleation of PE droplets [12]. In particular, PP lamellae become thicker with the decrease of the self-nucleation temperature from 170 °C to 161 °C. At the T_s 161 °C, the lamellar thickness of PP reached a maximum value, and consequently, the PE phase had the best nucleation substrate. However, depending on the PE type, a different nucleating effect of the PP matrix could be observed.

The cooling and heating scans corresponding to steps 5 and 6 in the applied self-nucleation thermal protocol (see Fig. 1) are shown in Fig. 4a–b, respectively, for a blend of PP with low-density polyethylene (LDPE922). The T_s range is selected to illustrate the temperature variations in the PP's crystallization and melting temperatures and to understand how the PE phase crystallization is influenced by the matrix self-nucleation. The self-nucleation domains of PP are identified by different curves' colours, i.e., *Domain I* red, *Domain II* blue, and *Domain III* green. Fig. 4a shows that while the crystallization temperature of PP has an obvious shift towards higher temperatures with decreasing T_s in *Domain II* and *III*, the peak from the PE minor phase remains approximately constant, at around 100 °C. Thus, enhanced surface nucleation does not seem particularly active for LDPE922, even when thicker PP lamellae (as judged by the higher melting point, Fig. 4b) are available at the interface with the molten PE phase.

Analogously, Fig. 5a–b report cooling and heating curves from various T_s for the PP/ZNPE935 blend. In this case, contrary to the previous example, the increase in PP crystallization temperature with decreasing T_s is accompanied by a significant increase in the crystallization temperature of the PE phase as well. As previously reported by our group, this behaviour indicates surface nucleation of PE on the PP matrix, which becomes more and more favourable with the thickening of the PP lamellae [12]. This surface nucleation mechanism is explained by the known epitaxial matching of PE crystals on PP substrates [8,41].

The recorded changes of PE phase crystallization temperature as a function of T_s for the two systems selected as examples (PP/LDPE922 and PP/ZNPE935) are reported in Fig. 6a–b, respectively. They are compared with the behaviour of the neat PE material and with the variation of the PP matrix crystallization temperature. In Fig. 6a, it can be seen that the increase of PE crystallization temperature (T_c) from T_s in PP *Domain I* (i.e., 225 °C) to *Domain III* (i.e., 161 °C) is practically negligible, although the shift in PP T_c is remarkable. On the other hand, the data for the blended PE present a characteristic trend displaying a minimum of T_c with T_s in the self-nucleation range of PP. The same trend is observed for all the materials that do not show meaningful surface nucleation effects, namely PP/mPE927, PP/mPE902 (see Supporting Information Figs. S4d and S4f, respectively). We note that the magnitude of the decrease in crystallization temperature is minimal (within 1 °C), nevertheless, the data are consistent and reproducible. The reason behind this result is currently unknown. However, it could be tentatively attributed to the generation of a particular state of the PP surface induced by self-nucleation, which is unfavourable for the nucleation of low-chain regularity PE (resulting in an anti-nucleation effect). The role of the interface here is deduced since the same dip in T_c values is not recorded for the neat PE material in the given T_s temperature range.

A different situation is depicted for high-chain regularity PEs (e.g., Fig. 6b). In this case, the T_c of the dispersed ZNPE935 phase increases by about 3 °C for T_s temperatures within PP *Domain II* and *III*, in correspondence with the increase in T_c of PP. On the other hand, the neat material does not show such variation in the same T_s temperature range, and the crystallization temperature starts to increase only at much lower temperatures, when the self-nucleation *Domain II* or *III* of the neat PE is encountered. This clearly indicates an interfacial interaction between PP and ZNPE935 by means of the known epitaxial nucleation mechanism, as already demonstrated for a similar PP/ZNPE blend in a previous work [12].

Fig. 7 reports the correlation between the dispersed phase's crystallization temperatures and the matrix with varying T_s in the PP self-nucleation domains for all the investigated blends. It can be observed that a linear relationship exists between the two T_c*s* for all the systems considered. However, the slope of the fitting lines is dependent on the PE chain regularity. In particular, the steepest slopes are obtained for the ZNPE with the higher densities, while the mPE and LDPEs are characterized by very low slopes. The data might be interpreted as a measure of the sensitivity of PE phase nucleation kinetics (as crystallization in the minor droplet phase is dominated by nucleation [14–17]) to a change in the matrix T_c. More precisely, being the T_c related to the undercooling and thus inversely related to the lamellar thickness, the link provided in Fig. 7 tells us how sensitive the crystallization of PE is to a change in PP lamellar thickness. In this respect, the largest effect on PE crystallization temperature is reported for ZNPE, while mPE and LDPE show almost no variation of their T_c with the change of PP's T_c. Therefore, mPE and LDPE are less sensitive to the PP surface. It is noteworthy that mPE918, despite the relatively low density, shows a mild surface nucleation effect. Therefore, density itself is apparently not the only controlling

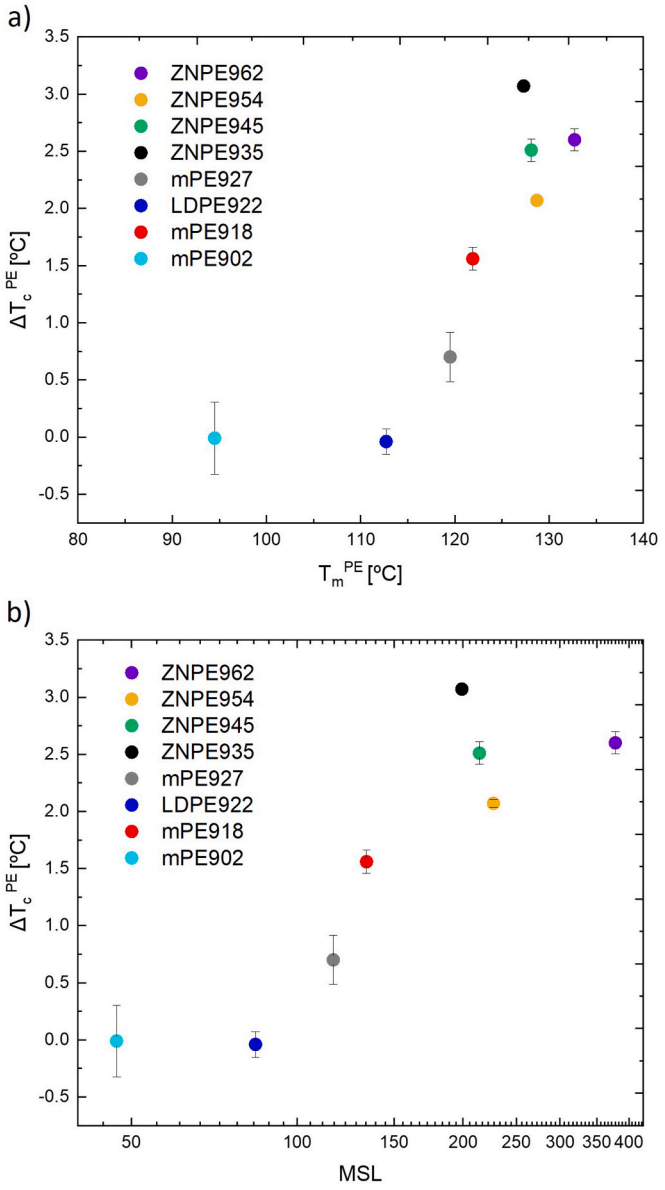

Fig. 8. Maximum increase in crystallization temperature recorded as a consequence of PP matrix self-nucleation for the different blends as a function of a) peak melting temperature and b) methylene sequence length of the various PE grades. The measurement error was estimated by repeating the measurement 6 times and employing the Student's t-distribution at a confidence level of 0.99 to calculate the error associated with a small number of repetitions.

aspect for surface nucleation.

We underline that the found scale of surface nucleation activity, i.e., high-density PE > linear low-density PE > low-density PE, is the same reported by Yan and Petermann in thin-films experiments. In their case, the epitaxially grown crystalline layer thickness decreases with a decrease in the PE density [11]. To explain this behaviour, two hypotheses can be put forward. On the one hand, the results point to the existence of a certain minimum chain regularity to allow surface nucleation of PE on PP, notwithstanding the lamellar thickness of the substrate. When there are too many chain defects (comonomer and/or branches), their presence hinders the templating of PE chains onto the PP substrate, thus disfavouring the nuclei formation. This latter case is analogous to the findings of Petermann and Yan on thin films of HDPE, LLDPE, and LDPE onto oriented PP [11]. A decrease in the epitaxial layer thickness was observed with decreasing PE density and interpreted as a competition between epitaxial nucleation and bulk (spherulitic) crystallization. Similarly, in our immiscible blends, nucleation at the surface might still be possible for the low-density materials. Still, the nucleation rate might be much slower with respect to that of HDPE, so eventually, it becomes comparable to or slower than the nucleation rate in the bulk of the PE droplets. On the other hand, Chaffin et al. reported that low chain regularity PEs could form entanglements easier with PP at the interface, [20] and that such topological constraints hinder epitaxial nucleation of the PE phase. Both hypotheses might play a role in our observations.

The overall surface nucleation effect of the different PE types can be obtained by considering the maximum increase in non-isothermal crystallization temperature between the melt cooled from the first T_s at which the crystallization temperature of the two phases does not overlap, i.e., 170 °C (edge of PP *Domain II*) and from PP *Domain III*, i.e., 161 °C.

The increase in crystallization temperature difference, calculated as outlined above, is plotted as a function of the peak melting temperature in Fig. 8a. T_m values and the surface nucleation effect of PE onto PP have a clear correlation. In particular, no enhanced nucleation effect is observed for T_m values lower than about 115 °C. When the T_m is larger than 120 °C, the increase in the T_c of the PE phase starts to be larger than 1 °C, and afterwards it increases approximately linearly with the melting temperature. Generally speaking, the higher the T_m value, the longer the uninterrupted crystallizable PE chain sequence is. Fig. 8a suggests that a certain level of PE chain regularity is required to enable efficient surface-induced nucleation of PE onto PP in immiscible blends. The behaviour of mPE918 is noteworthy, as it displays a low density but melting temperature higher than grades with similar densities. This data is thus corroborating the fact that melting temperature is governing surface-nucleation of PE onto PP, rather than the sole density.

The PE chain regularity can be represented by the value of the methylene sequence length (MSL), calculated from the melting point of the polyethylene grade. As melting temperatures of ethylene copolymers decrease with the increase in branch content but are independent of the

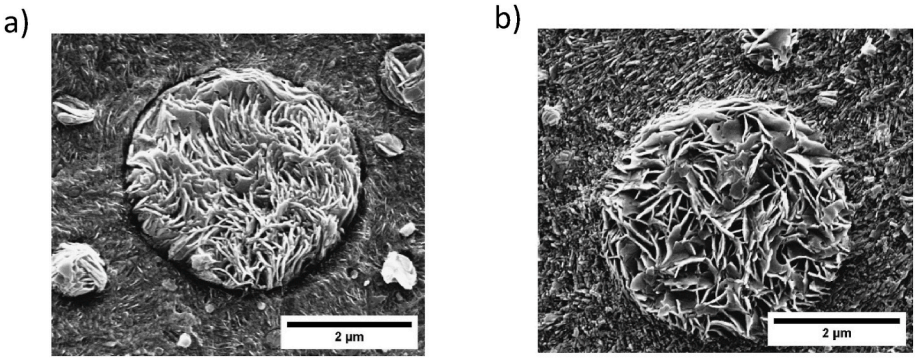

Fig. 9. SEM images of the PP/ZNPE935 blend after cooling from selected T_s: a) T_s 225 °C, b) 161 °C.

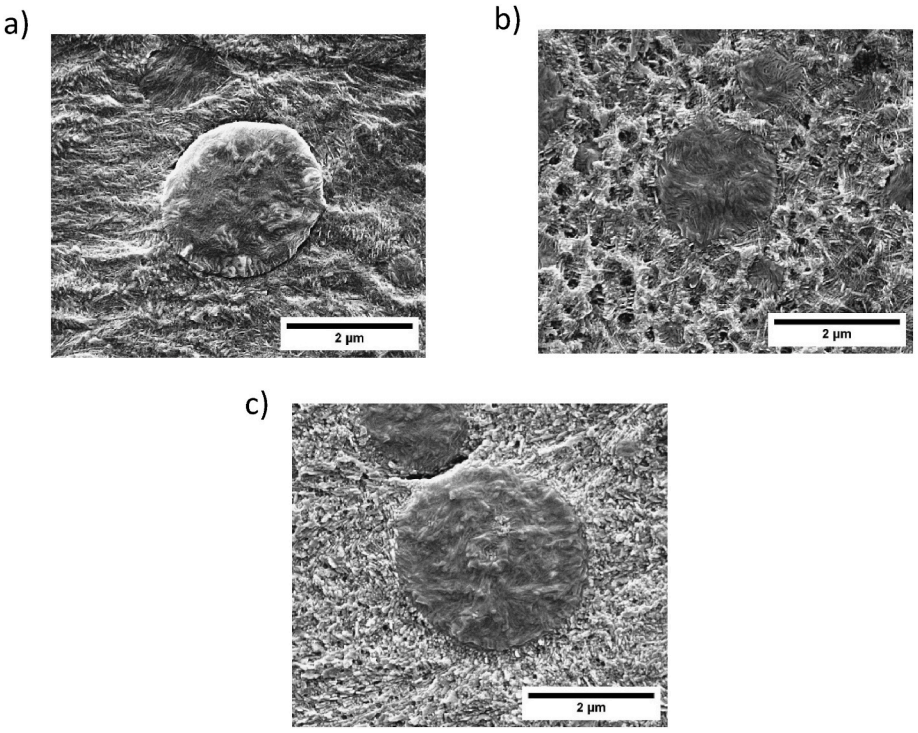

Fig. 10. SEM images of the PP/LDPE922 blend after cooling from selected T_s first images (a) T_s 225 °C b) 167 °C, c) 161 °C.

branch length [42,43], it is convenient to consider this parameter. MSL could be calculated in relation to the change in melting temperature of the polyethylene grade according to empirical relations such as the one reported in Equation (2) [44–46].

$$MSL = \frac{2}{e^{\left(\frac{142.2}{T_m[K]} - 0.3451\right)} - 1} \quad (2)$$

The relation between the maximum increase of crystallization temperature of the PE phase and MSL could be appreciated again in Fig. 8b. No enhanced nucleation effect is observed for MSL values lower than about 100. After a threshold value of 200, the increase in T_c reaches a plateau. It should be noted that the reported MSL values, being related to the peak melting temperature, only represent the most probable MSL among the polymer chains and not the average or the maximum. It is also clear that, since it is based on an empirical relation derived for long alkanes (equation (2)), the calculated MSL could deviate from the real values, as determined for instance via NMR. Nevertheless, the conclusions on chain regularity effect on surface nucleation of PE onto PP that can be grasped from Fig. 8b can be considered as semi-quantitative.

In order to demonstrate that nucleation of PE droplets occurred at the interface with the PP matrix and to different extents for the PE grades of varying regularity, SEM analysis on thermally treated and etched samples was conducted. The results are shown in Figs. 9 and 10. Fig. 9 shows the detail of a single ZNPE935 droplet embedded in the PP matrix, crystallized starting from a T_s temperature in PP *Domain I* (Fig. 9a) or *Domain III* (Fig. 9b). In both cases, there is a relevant fraction of PE lamellar stacks which originate from the droplet interface. However, in the case of the lower seeding temperature (Fig. 9b), the nucleation density at the droplet surface is higher, leading to the generation of a transcrystalline morphology. This indicates the promoted surface nucleation in the case of high-density ZNPE. The results are analogous to previous observations on a similar system, constituted by a blend of the same PP matrix and a Ziegler-Natta PE with a slightly higher density (945 kg/m^3) [12].

To investigate the peculiar minimum in T_c versus T_s for PP/LDPE922 blends, samples were pre-treated in the DSC to obtain PP in *Domain I*, *Domain II* and *Domain III* at 225 °C, 167 °C and 161 °C, respectively. The droplets of LDPE appear to be darker than the PP matrix. In Fig. 10a, a relatively smooth interface between the two phases can be appreciated, while the main nucleation sites of the LDPE are difficult to be detected since the lamellar stacks seem to originate from both the bulk and the interface of the droplet. In Fig. 10b, the phase boundary becomes rougher due to the higher amount of spherulites that were created during self-nucleation of the PP matrix. On the other hand, at T_s = 161 °C (Fig. 10c), a smoother interface is again obtained because the PP matrix is just partially molten and annealed during the thermal treatment. Therefore, the observed minimum in T_c with T_s can be tentatively attributed to a change in the roughness state of the PP/PE surface. Similar changes can be highlighted in another system displaying the same minimum, i.e., PP/mPE902, see Figs. S3f and S4, where the very low-density PE phase has been etched away before the SEM measurement. We note that if the surface roughness plays a role in the observed decrease of the overall crystallization kinetics at intermediate T_ss, it must mean that nucleation occurs at the interface, at least to some extent, and also for the materials with lower chain regularity. However, the fact that the T_c is not increased when changing the lamellar thickness of the PP substrate points towards the fact that the surface nucleation mechanism is not dominant in these PEs, and it must be competing with nucleation in the bulk of the droplet.

In fact, by comparing Figs. 9b and 10c, it can be seen that a transcrystalline layer at the interface is clearly apparent for the ZNPE sample annealed at 161 °C, while it is practically absent for the LDPE sample. This is in agreement with the measurement by Petermann and Yan, which observed a large decrease of the PE epitaxial layer thickness onto PP substrates when passing from HDPE to LDPE [11].

4. Conclusions

We previously reported that surface nucleation of polyethylene droplets at the interface with polypropylene matrix is promoted by the self-nucleation of the PP matrix in PP/PE blends. In this work, we investigated the effect of the PE phase chain regularity on the mechanism of epitaxial crystallization onto the self-nucleated PP matrix.

We found that the surface nucleation of PE droplets on self-nucleated PP matrices, strongly depends on chain regularity. Thus the increase in crystallization temperature observed for PE droplets (that correlates with an increase in nucleation effect) was maximum for HDPE samples, much less for metallocene-catalyzed LLDPE, and negligible for highly branched and comonomer-rich polymers.

The results were interpreted by considering polymer chain regularity, i.e., the average methylene sequence length (MSL), as a key parameter. It was noted that when the PE crystallizable sequence length is below ~100, corresponding to a melting temperature lower than approximately 115 °C, the epitaxial matching between the aligned PE chains and the rows of PP methyl groups can not be efficiently attained, and the surface nucleation rate dramatically slows down. The increase in interfacial entanglement between PE and PP with decreasing PE regularity could also possibly hinder epitaxial crystallization among the two polymers.

Electron microscopy observations corroborate the DSC results, as a distinct interfacial morphology could be detected in HDPE and LDPE samples, with the latter lacking a clear transcrystalline layer, which is instead observed for the former polymer pair.

Funding

This work has received funding from the European Union's Horizon 2020 research and innovation programme under the Marie Sklodowska-Curie grant agreement No. 860221. AJM acknowledges funding from the Basque Government through grant IT1503-22.

CRediT authorship contribution statement

Magdalena Góra, Sebastián Coba-Daza: experiments, data analysis

Magdalena Góra: writing first draft

Enrico Carmeli,Davide Tranchida, Andreas Albrecht, Alejandro Müller, Dario Cavallo: experimental design and draft manuscript revision

Dario Cavallo: conceptualization and supervision

Declaration of competing interest

The authors declare that they have no known competing financial interests or personal relationships that could have appeared to influence the work reported in this paper.

Data availability

Data will be made available on request.

Acknowledgements

The authors thank Stefanie Strauss for her support in performing TREF and GPC measurements, and to Philipp Schwarz for his support in conducting the WAXS measurements.

Appendix A. Supplementary data

Supplementary data to this article can be found online at https://doi.org/10.1016/j.polymer.2023.126180.

References

[1] F.P. Price, Nucleation in Polymer Crystallization. Nucleation, Marcel Dekker, Inc, 1969.
[2] B. Wunderlich, Structural data on crystalline polymers by thermal analysis, J polym sci, C Polym symp. 43 (2007) 29–42.
[3] M. Gahleitner, J. Wolfschwenger, D. Mileva, Polymer Crystal Nucleating Agents. Reference Module in Materials Science and Materials Engineering, Elsevier, 2016, B9780128035818037000.
[4] Z. Guo, R. Xin, J. Hu, Y. Li, X. Sun, S. Yan, Direct High-Temperature Form I Crystallization of Isotactic Poly(1-Butene) Assisted by Oriented Isotactic Polypropylene, 8, 2019.
[5] J.C. Wittmann, B. Lotz, Epitaxial crystallization of polymers on organic and polymeric substrates, Prog. Polym. Sci. 15 (1990) 909–948.
[6] H. Zhou, S. Jiang, S. Yan, Epitaxial crystallization of poly(3-hexylthiophene) on a highly oriented polyethylene thin film from solution, J. Phys. Chem. B 115 (2011) 13449–13454.
[7] B. Lotz, J.C. Wittmann, Structural relationships in blends of isotactic polypropylene and polymers with aliphatic sequences, J. Polym. Sci. B Polym. Phys. 24 (1986) 1559–1575.
[8] B. Lotz, J.C. Wittmann, Polyethylene–isotactic polypropylene epitaxy: analysis of the diffraction patterns of oriented biphasic blends, J. Polym. Sci. B Polym. Phys. 25 (1987) 1079–1087.
[9] S. Yan, J. Petermann, D. Yang, Effect of lamellar thickness on the epitaxial crystallization of PE on oriented iPP films, Polym. Bull. 38 (1997) 87–94.
[10] S. Yan, D. Yang, J. Petermann, Controlling factors for the occurrence of heteroepitaxy of polyethylene on highly oriented isotactic polypropylene, Polymer 39 (1998) 4569–4578.
[11] S. Yan, J. Lin, D. Yang, J. Petermann, Critical epitaxial layers of different kinds of polyethylene on highly oriented isotactic poly(propylene) substrates, Macromol. Chem. Phys. 195 (1994) 195–201.
[12] E. Carmeli, S.E. Fenni, M.R. Caputo, A.J. Müller, D. Tranchida, D. Cavallo, Surface nucleation of dispersed polyethylene droplets in immiscible blends revealed by polypropylene matrix self-nucleation, Macromolecules 54 (2021) 9100–9112.
[13] W. Wang, S. Buzzi, S.E. Fenni, E. Carmeli, B. Wang, G. Liu, et al., Surface nucleation of dispersed droplets in double semicrystalline immiscible blends with different matrices, Macromol. Chem. Phys. (2022), 2200202.
[14] M.E. Córdova, A.T. Lorenzo, A.J. Müller, L. Gani, S. Tencé-Girault, L. Leibler, The influence of blend morphology (Co-continuous or sub-micrometer droplets dispersions) on the nucleation and crystallization kinetics of double crystalline polyethylene/polyamide blends prepared by reactive extrusion: the influence of blend morphology (Co-continuous or sub-micrometer droplets dispersions), Macromol. Chem. Phys. 212 (2011) 1335–1350.
[15] B. Wang, R. Utzeri, M. Castellano, P. Stagnaro, A.J. Müller, D. Cavallo, Heterogeneous nucleation and self-nucleation of isotactic polypropylene microdroplets in immiscible blends: from nucleation to growth-dominated crystallization, Macromolecules 53 (2020) 5980–5991.
[16] S.E. Fenni, A.J. Müller, D. Cavallo, Understanding polymer nucleation by studying droplets crystallization in immiscible polymer blends, Polymer 264 (2023), 125514.
[17] L. Sangroniz, B. Wang, Y. Su, G. Liu, D. Cavallo, D. Wang, et al., Fractionated crystallization in semicrystalline polymers, Prog. Polym. Sci. 115 (2021), 101376.
[18] B. Fillon, J.C. Wittmann, B. Lotz, A. Thierry, Self-nucleation and recrystallization of isotactic polypropylene (α phase) investigated by differential scanning calorimetry, J. Polym. Sci. B Polym. Phys. 31 (1993) 1383–1393.
[19] S.E. Fenni, M.R. Caputo, A.J. Müller, D. Cavallo, Surface roughness enhances self-nucleation of high-density polyethylene droplets dispersed within immiscible blends, Macromolecules 55 (2022) 1412–1423.
[20] K.A. Chaffin, F.S. Bates, P. Brant, G.M. Brown, Semicrystalline blends of polyethylene and isotactic polypropylene: improving mechanical performance by enhancing the interfacial structure, J. Polym. Sci. B Polym. Phys. 38 (2000) 108–121.
[21] B.C. Poon, S.P. Chum, A. Hiltner, E. Baer, Adhesion of polyethylene blends to polypropylene, Polymer 45 (2004) 893–903.
[22] A.M. Jordan, K. Kim, D. Soetrisno, J. Hannah, F.S. Bates, S.A. Jaffer, et al., Role of crystallization on polyolefin interfaces: an improved outlook for polyolefin blends, Macromolecules 51 (2018) 2506–2516.
[23] International A, D1601 - 20 Standard Test Method for Analysis of Ethylene Glycols and Propylene Glycols by Gas Chromatography, Internet, 2023. Available from: https://www.astm.org/standard/D1601.html.
[24] R.M. Michell, A. Mugica, M. Zubitur, A.J. Müller, Self-nucleation of crystalline phases within homopolymers, polymer blends, copolymers, and nanocomposites, in: F. Auriemma, G.C. Alfonso, C. de Rosa (Eds.), Polymer Crystallization I, Springer International Publishing, Cham, 2015. . pp. 215–56.
[25] L. Sangroniz, D. Cavallo, A.J. Müller, Self-nucleation effects on polymer crystallization, Macromolecules 53 (2020) 4581–4604.
[26] D.R. Gee, T.P. Melia, Thermal properties of melt and solution crystallized isotactic polypropylene, Makromol. Chem. 132 (1970) 195–201.
[27] F.J. Lanyi, N. Wenzke, J. Kaschta, D.W. Schubert, On the determination of the enthalpy of fusion of α-crystalline isotactic polypropylene using differential scanning calorimetry, X-ray diffraction, and fourier-transform infrared spectroscopy: an old story revisited, Adv. Eng. Mater. 22 (2020), 1900796.
[28] B. Wunderlich, G. Czornyj, A study of equilibrium melting of polyethylene, Macromolecules 10 (1977) 906–913.
[29] F.M. Mirabella, A. Bafna, Determination of the crystallinity of polyethylene/?-olefin copolymers by thermal analysis: relationship of the heat of fusion of 100% polyethylene crystal and the density, J. Polym. Sci. B Polym. Phys. 40 (2002) 1637–1643.
[30] H.M. Ayad Mr Ahmed, M.A. Abou-El-Enein, Crystallization behavior and thermal properties of polypropylene/high-density polyethylene blends, J. Appl. Polym. Sci. 119 (2011) 3202–3210.
[31] J.K. Gill, Blends of polypropylene and polyethylene: morphology and properties, Polymer 35 (1994) 794–803.
[32] J. Balakrishnan, S.S. Sadasivuni, Polypropylene/polyethylene blends: structure, properties, and processing, Polym.-Plast. Technol. Eng. 48 (2009) 413–432.

[33] E. Carmeli, G. Kandioller, M. Gahleitner, A.J. Müller, D. Tranchida, D. Cavallo, Continuous cooling curve diagrams of isotactic-polypropylene/polyethylene blends: mutual nucleating effects under fast cooling conditions, Macromolecules 54 (2021) 4834–4846.
[34] S.E. Fenni, M. Spigno, W. Wang, A. Costanzo, A.J. Müller, D. Cavallo, How nucleating particles migration affects the fractionated crystallization of isotactic polypropylene/polystyrene immiscible blends, Thermochim. Acta 719 (2023), 179407.
[35] Z. Bartczak, A. Galeski, M. Pracella, Spherulite nucleation in blends of isotactic polypropylene with high-density polyethylene, Polymer 27 (1986) 537–543.
[36] A. Gałeski, Z. Bartczak, M. Pracella, Spherulite nucleation in polypropylene blends with low density polyethylene, Polymer 25 (1984) 1323–1326.
[37] K. Matyjaszewski, M. Möller (Eds.), Polymer Blends: Preparation, Properties, and Applications, John Wiley & Sons, 2006.
[38] B. Nebe (Ed.), Handbook of Polymer Synthesis, Characterization, and Processing, Springer, 2017.
[39] M.L. Arnal, M.E. Matos, R.A. Morales, O.O. Santana, A.J. Müuller, Evaluation of the fractionated crystallization of dispersed polyolefins in a polystyrene matrix, Macromol. Chem. Phys. 199 (1998) 2275–2288.
[40] S. Chandrasekhar, Stochastic problems in Physics and astronomy, Rev Mod Phys. American Physical Society 15 (1943) 1–89.
[41] S. Yan, D. Yang, Critical crystallization temperature for the occurrence of epitaxy between high-density polyethylene and isotactic polypropylene, J. Appl. Polym. Sci. 66 (1997) 2029–2034.
[42] R.G. Alamo, L. Mandelkern, Thermodynamic and structural properties of ethylene copolymers, Macromolecules 22 (1989) 1273–1277.
[43] R.G. Alamo, B.D. Viers, L. Mandelkern, Phase structure of random ethylene copolymers: a study of counit content and molecular weight as independent variables, Macromolecules 26 (1993) 5740–5747.
[44] M. Keating, I.-H. Lee, C.S. Wong, Thermal fractionation of ethylene polymers in packaging applications, Thermochim. Acta 284 (1996) 47–56.
[45] M. Zhang, S.E. Wanke, Quantitative determination of short-chain branching content and distribution in commercial polyethylenes by thermally fractionated differential scanning calorimetry, Polym. Eng. Sci. 43 (2003) 1878–1888.
[46] A.T. Lorenzo, M.L. Arnal, A.J. Müller, A. Boschetti de Fierro, V. Abetz, High speed SSA thermal fractionation and limitations to the determination of lamellar sizes and their distributions, Macromol. Chem. Phys. 207 (2006) 39–49.